Why dip moveout ?

Shuki Ronen and Fabio Rocca

Abstract

CDP stacking after NMO reduces the amplitudes of both random noise and reflections with other stacking velocity. However, the signal is spatially smoothed and disturbances due to aliasing noise and side diffractions are not completely removed.

The signal can be partially restored by post-stack inverse filtering, but at the cost of decreasing the overall signal-to-noise ratio. We show that dip moveout and weighted stack (equivalent to non-uniform offset spacing) reduce coherent and aliasing noise, even if the dip moveout correction is not completely accurate.

Introduction: the concept of dip moveout

Conventionally, we migrate zero offset sections that we get from the non zero offset seismic data by normal moveout (NMO) correction. However, it is well known (Levin, 1971) that in a common midpoint gather the moveout Δt of a reflection from a plane reflector in a constant velocity medium is given by:

$$\Delta t = t_0 \left[\sqrt{1 + \frac{4h^2}{v^2 t_0} \cos^2\theta} - 1 \right] \qquad (1)$$

$$\approx \frac{2h^2}{v^2 t_0} \cos^2\theta$$

In equation (2), t_0 is the zero-offset arrival time. The half-offset h and the dip angle θ are shown in Figure 1; v is the velocity. The approximation is for small offset angle $h \ll vt_0$, i.e. below the mute.

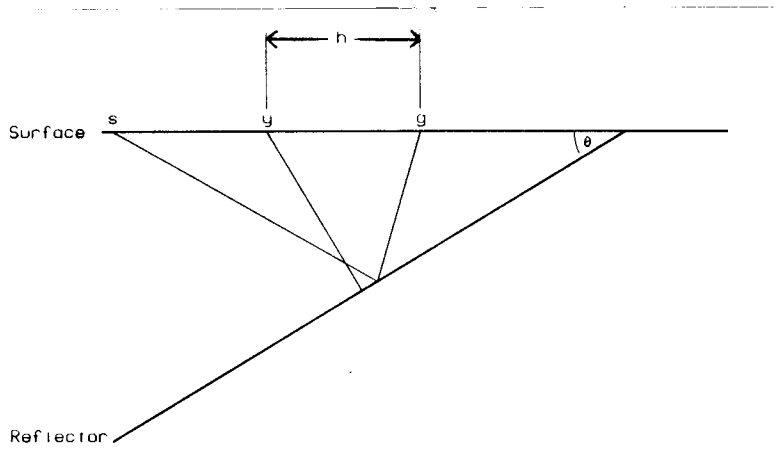

FIG. 1. Dipping reflector: the moveout is less then the NMO.

The moveout is decomposed into normal moveout Δt_N and dip moveout (DMO) Δt_D:

$$\Delta t = \Delta t_N - \Delta t_D$$

If we want to reconcile data coming from different common offset sections we have to correct them for both NMO and DMO. While the NMO correction is only a time stretch, the dip moveout correction implies a time varying spatial filter. This latter operation is usually known as Pre Stack Partial Migration and has been discussed by several authors (Sherwood et al., 1976; Yilmaz and Claerbout, 1980; Ottolini, 1981; Hale, 1982; Deregowski and Rocca, 1982; Bolondi et al., 1982). A more detailed geometrical analysis of the dip moveout correction and stack is presented in the companion paper "Stacking Smiles" in this report. Referring to the previous papers for detailed proofs, we will start here with the formula:

$$P_h(k,\omega) \approx \exp\left[i\,\omega\,\frac{2h^2}{v^2 t_0}\right] \exp\left[-i\,\frac{h^2 k_y^2}{2\omega t_0}\right] \cdot P_0(k,\omega) \qquad (2)$$

that gives the relation between $P_h(k,\omega)$, the two dimensional Fourier transform of the section having common offset $2h$, and the zero offset section $P_0(k,\omega)$. Equation (2) is derived from (1) with small offset angle approximation; $h \ll vt_0$. The first exponent is the NMO and

the second is the dip moveout. The NMO does not depend directly on the midpoint y (only through lateral velocity variation); the DMO is dependent on k_y and is velocity independent, enabling processing before velocity analysis. Equation (2) contains both time t_0 and temporal frequency ω, since the operator is time varying. However, it is known that this is acceptable, since the variation of the operator in its time span is small, at least whenever h is smaller than $vt_0/2$.

Surface side diffractors

In a recent paper (Larner et al.,1982), an exhaustive explanation has been proposed for the origin of one kind of a coherent noise in marine data. The authors have shown that this noise is mostly due to side scatterers on the sea bottom. When the scatterer lies amidship (position a in Figure 2) the reflection has no dip moveout and therefore stacks at water velocity. However, since the location may be far aside, the arrival time may be the same as that of reflections coming from below. The stack is carried out with the rock velocity, much higher than that of the water and these side reflections stack out.

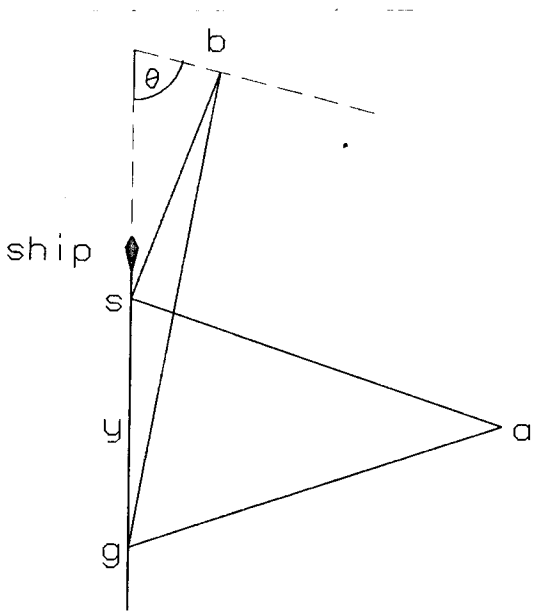

FIG. 2. A side diffractor on a CMP gather can appear as a hyperbola like event a, or as a "flat top" like event b. Event a will stack out, event b will stack in if we carry out NMO only, with the velocity of the rocks at the correspondent depth.

The contrary will happen for reflector b that lies forward (or after) the ship. In this case, the apparent dip θ of the reflection is high, and therefore the operations of NMO and stack at sediment velocity will not be able to remove the reflections. Events like b stack in and will appear as slanting stripes on the stacked section.

In other words, the hyperbolic diffraction pattern will disappear after stack, only where its time slope is small enough so that the apparent dip $\theta = \arcsin\left[\frac{v}{2}\frac{dt}{dy}\right]$ is also small. All this is explained by the equations:

$$Stack_a \approx \sum_h \exp\left[i\omega \frac{2h^2}{t_0}\left(\frac{1}{v_w^2} - \frac{1}{v_r^2}\right)\right] \cdot P_0$$

$$Stack_b \approx \sum_h \exp\left[i\omega \frac{2h^2}{t_0}\left(\frac{\cos^2\theta}{v_w^2} - \frac{1}{v_r^2}\right)\right] \cdot P_0$$

where P_0 is the zero-offset section v_r and v_w are the sediment and water velocity respectively and θ is the apparent dip angle of the reflection. The approximation is for small offset angle. The phasors in equation (2) will stack in phase if the exponent is small enough and this might happen for sufficiently high values of θ. It is clear that, had we corrected for dip moveout, all reflections from side diffractors would have been canceled:

Spatial aliasing and offset

The wavefield recorded in a seismic experiment is sampled both in time and space. Before sampling the data are lowpass filtered in time to avoid aliasing. A time filter is inexpensive and easy to apply ahead of the A/D converter.

The same should be done before spatial sampling, and it is partially done with patterns of phones and arrays of sources. However, some aliasing is unavoidable, particularly of cable noise; If the maximum signal frequency is 70 Hz, then waves traveling horizontally in the water will have a wavelength of about 20 m. If the midpoint spacing is 25 m the cable noise will be badly aliased, (especially events like b in Figure 2).

This might make doubtful the success of DMO correction; fortunately, it is not so as we will see. In fact, we will show that we will be able to recover the full spatial resolution of the signal.

Due to spatial aliasing and using equation (2), the data we actually have, a sampled version of the common offset section, is $P_h^{(s)}$:

$$P_h^{(s)}(k) = \sum_{n=-\infty}^{\infty} P_h(k - nk_0) \qquad (3)$$

$$= \exp\left[i\omega \frac{2h^2}{v^2 t_0} \right] \sum_{n=-\infty}^{\infty} \exp\left[-i \frac{h^2 k_0^2}{2\omega t_0} \left(\frac{k}{k_0} - n \right)^2 \right] P_0(k - nk_0)$$

where $k_0 = 2\pi/\Delta y$ is the sampling wavenumber, $P_h(k)$ is the constant offset section we would have with infinitesimal midpoint spacing.

Conventional stacking without dip moveout

Using equation (3) we can show the effects of ignoring DMO, i.e. of conventional processing in the presence of simultaneous contradictory dips. It is important to remember, though, that if only one dip is present, conventional processing will alter the stacking velocity by the cosine of the dip and there will be no reduction of spatial resolution. The velocity however will be incorrect. In the following we will assume correct NMO and no DMO at all.

Normal moveout removes the first exponent in (3); stacking will give:

$$Stack = \sum_h \exp\left[-i \frac{h^2 k^2}{2\omega t_0} \right] P_0(k) \qquad (4)$$

$$+ \sum_{n=1}^{\infty} \sum_h \exp\left[-i \frac{h^2 k_0^2}{2\omega t_0} \left(\frac{k}{k_0} \pm n \right) \right] P_0(k \pm nk_0)$$

The stacked section is still different from the zero-offset section P_0 due to the aliasing noise; moreover the signal is distorted by the function:

$$F = \sum_h \exp\left[-i \frac{h^2 k^2}{2\omega t_0} \right] \qquad (5)$$

We have not yet defined how to sum over the offsets. If there are m geophones, uniformly spaced along the cable, and assuming $\Delta h = \Delta y$, we replace the j-th hk_0 in equation (5) by $j2\pi$. Summing with equal weights we have:

$$F = \frac{1}{m} \sum_{j=0}^{m-1} \exp\left[-i \frac{2\pi^2}{\omega t_0} \left(\frac{k}{k_0} \right)^2 j^2 \right] \qquad (6)$$

As can be seen in Figure 3 the signal distortion is not drastic. Most of our data are in the high flat area of F that drops in the evanescent and horizontal waves zones.

Another possibility for stacking is to make constant the difference between the squares of the offsets. This corresponds to weighting less the inner offsets and more the

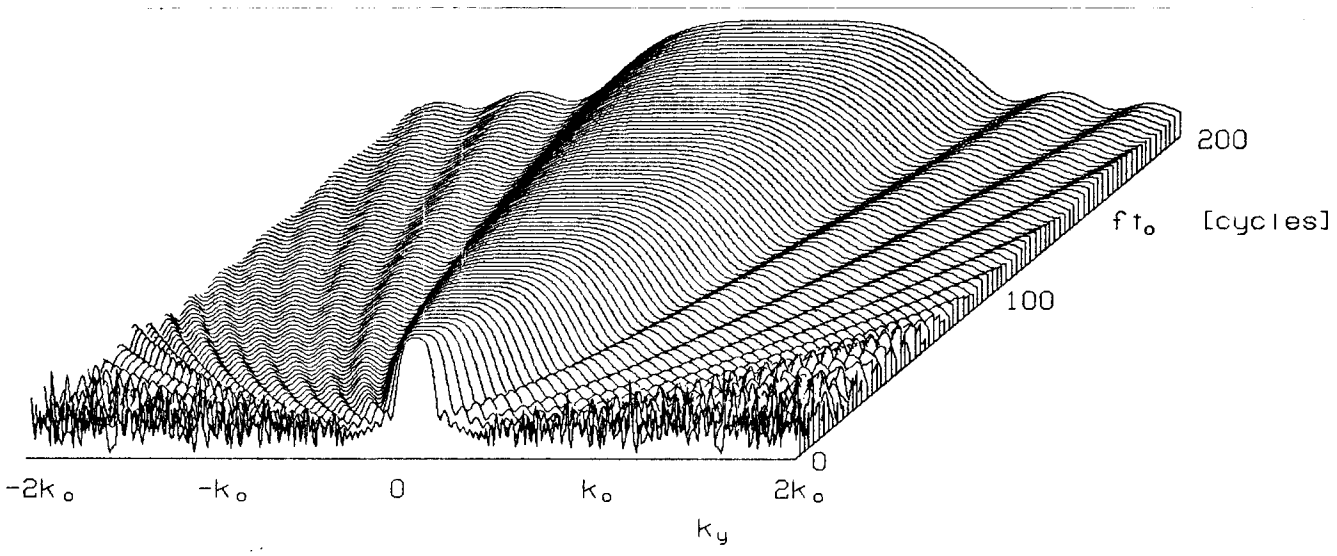

FIG. 3. F without DMO. Uniform h.

outer ones. It is actually done when multichannel filters are used for the removal of particularly troublesome multiples. Taking Uniform Offset Squares (UOS) we reduce the number of channels we use, from m to N UOS channels. The j'th h^2 is $(m\Delta h)^2 j/N$. We replace $(h^2 k_0^2)$ in equation (5) by $4\pi^2 m^2 j/N$ and we find F to be:

$$F = \frac{1}{N}\sum_{j=0}^{N-1} \exp\left[-i\,\frac{2\pi^2 m^2}{\omega t_0 N}\left(\frac{k}{k_0}\right)^2 j\right] \tag{7}$$

$$= \frac{1}{N}\,\frac{1-\exp\left[-i\,\Phi\,(N+1)\right]}{1-\exp\left[-i\,\Phi\right]}$$

Where:

$$\Phi = \frac{2\pi^2 m^2}{\omega t_0 N}\left(\frac{k}{k_0}\right)^2$$

F with UOS is presented in Figure 4: The deviation from a constant is worse than that of uniform offset stacking (Figure 3) expressing the fact that with UOS we rely more on far offsets which are not moved out properly. F will get better (i.e. more constant) the less we use the far offsets.

In equation (5) we would like F to be a constant. To obtain that we might spatially deconvolve the signal *after stack*. This "After Stack Dip Moveout" would be able to restore the signal, but would also increase the noise where F is small.

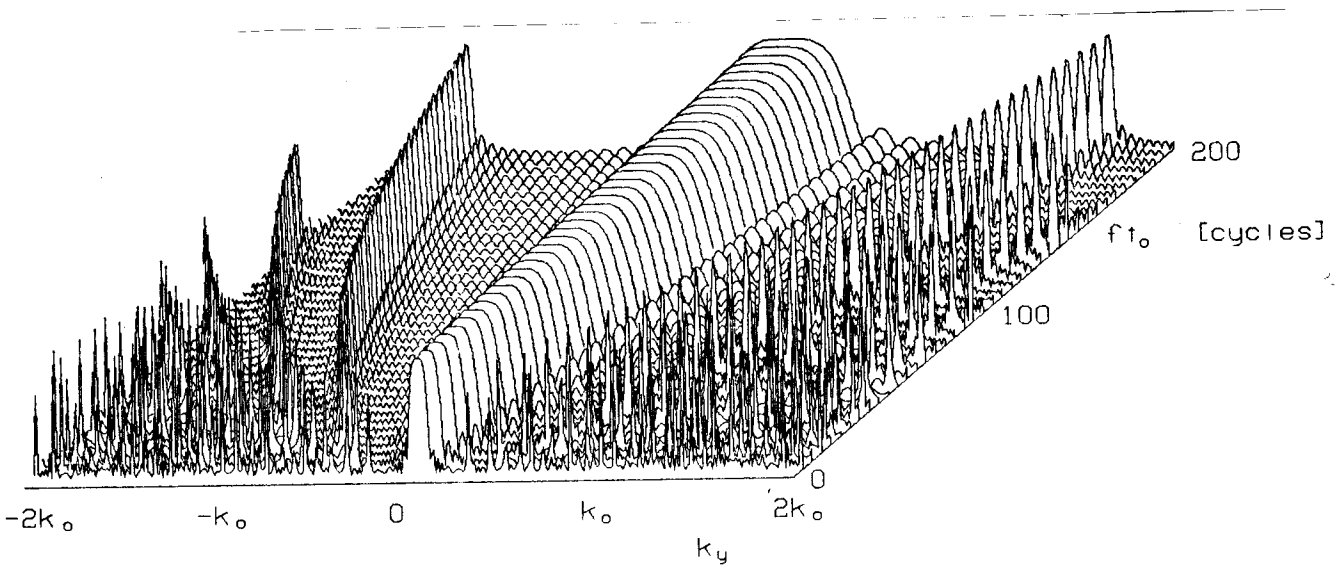

FIG. 4. F without DMO. Uniform h^2.

Stacking after DMO and NMO

If we carry out DMO and NMO, the output of the prestack process from each constant offset section is:

$$P_0{}^{(s)}(k) = P_h^{(s)}(k) \exp\left[i \frac{h^2 k^2}{2\omega t_0} \right] \tag{8}$$

$$= \sum_n P_h(k - nk_0) \exp\left[i \frac{h^2 k^2}{2\omega t_0} \right]$$

$$= \sum_n P_h(k - nk_0) \exp\left[- i \frac{h^2 k_0^2}{2\omega t_0} \left(\frac{k}{k_0} - n \right)^2 \right] \exp\left[i \frac{h^2 k^2}{2\omega t_0} \right]$$

$$= \sum_n P_h(k - nk_0) \exp\left[- i \frac{h^2 k_0^2}{2\omega t_0} n \left(n - \frac{2k}{k_0} \right) \right]$$

The stack will be:

$$Stack(k) = \sum_h P_0{}^{(s)}(k) \tag{9}$$

$$= \sum_{n=-\infty}^{\infty} P_0(k - nk_0) \sum_h \exp\left[- i \frac{h^2 k_0^2}{2\omega t_0} n \left(n - \frac{2k}{k_0} \right) \right]$$

$$= \sum_{n=-\infty}^{\infty} P_0(k - nk_0)\, F_n(k)$$

where:

$$F_n(k) = \sum_h \exp\left[-i \frac{h^2 k_0^2}{2\omega t_0} n \left(n - \frac{2k}{k_0} \right) \right] \tag{10}$$

In equation (9) the signal is not distorted at all. This happens because we modeled the DMO using the same expression (except the sign) that we used for its correction. Actually, the DMO correction is only an approximation; but we know already from Figure 3 that this residual distortion is negligible. In fact, the distortion without any correction at all was already small. The good news is that the aliased components in equation (9) are multiplied by a sum of phasors, generally out of phase; thus, aliasing noise will be reduced except when $k = nk_0/2$. As it is shown in the companion paper, this exception and cannot be avoided, even when using better approximations of the DMO.

Ideally, $F_n(k) = \delta(n)$, independent of all the other variables; the actual F depends on how we sum over h. If we stack with uniform offset we get:

$$F_n(k) = \frac{1}{m} \sum_{j=0}^{m-1} \exp\left[-i \frac{2\pi^2}{\omega t_0} n \left(n - \frac{2k}{k_0} \right) j^2 \right] \tag{11}$$

as described in Figure 5 for $m = 48$. If we use $m = 16$ to save in DMO operations, we get Figure 6.

If we stack with UOS F_n will be:

$$F_n(k) = \frac{1}{N} \sum_{j=0}^{N} \exp\left[-i\, \Phi_n(k, \omega t_0)\, j \right] \tag{12}$$

$$= \frac{1}{N} \frac{1 - e^{i(N+1)\Phi}}{1 - e^{i\Phi}}$$

where:

$$\Phi_n(k, \omega t_0) = n \left(n - \frac{2k}{k_0} \right) \frac{2\pi^2 m^2}{N \omega t_0} \tag{13}$$

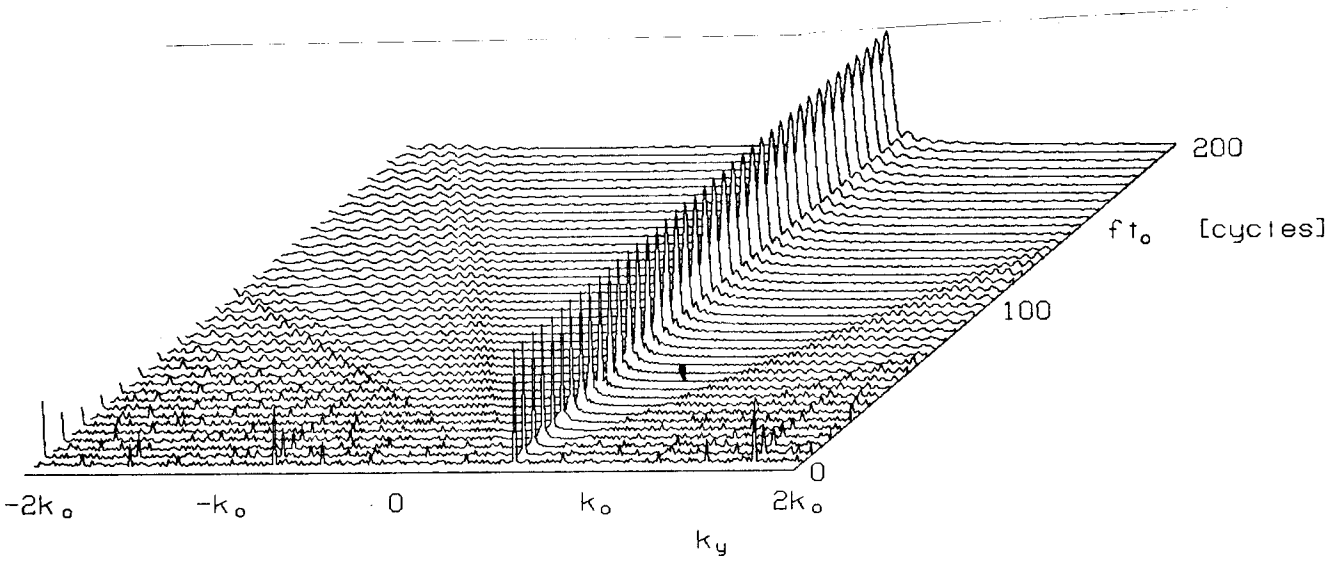

FIG. 5. $F_n(k)$, $(n = 1)$, uniform offset spacing, $m = 48$.

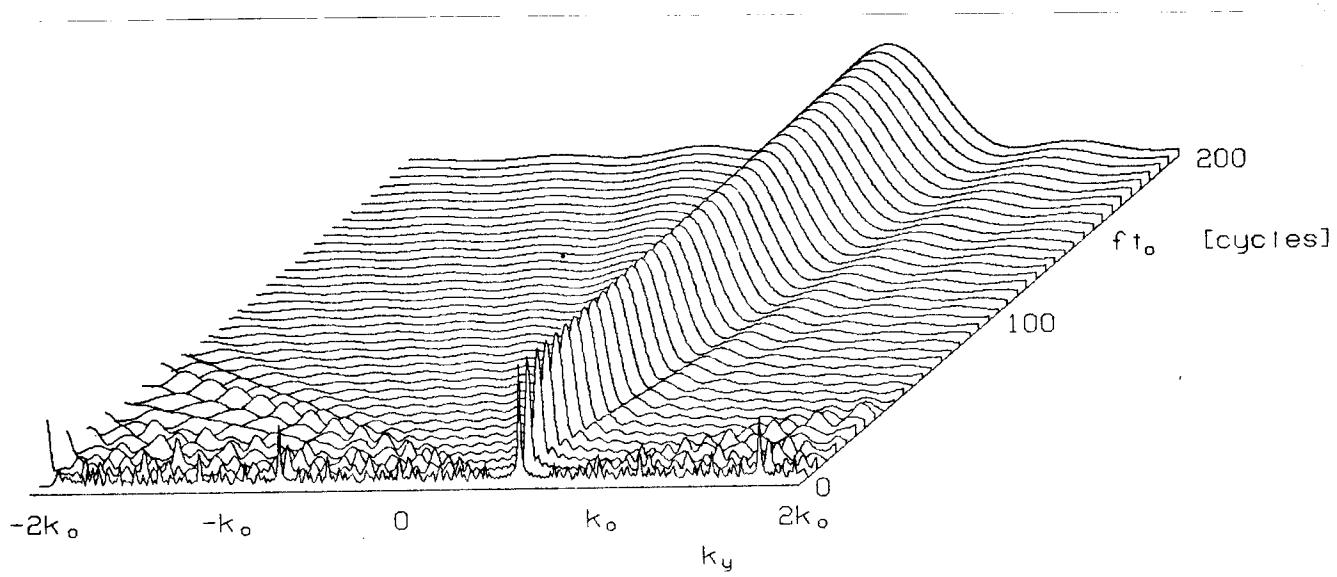

FIG. 6. $F_n(k)$, $(n = 1)$, uniform offset spacing, $m = 16$.

The result is illustrated by Figures 7 and 8: We get better results with UOS (after dip moveout !), as can be seen comparing Figures 6 and 8. Figure 8 has additional peaks, but they are narrow and the total energy is less. A more complete comparison is shown in Figures 11 through 14. The clip value for Figures 11 and 12 is the same, likewise for Figures 13 and 14. The total alias energy is the significant parameter.

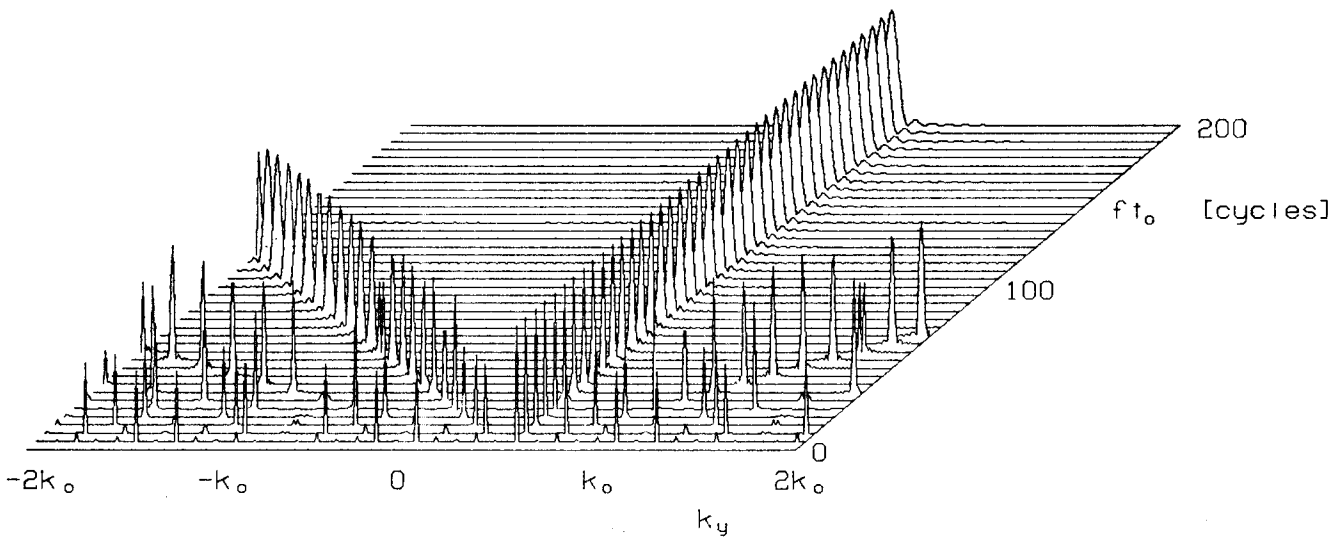

FIG. 7. $F_n(k)$, $(n = 1)$, UOS spacing, $N = 48$.

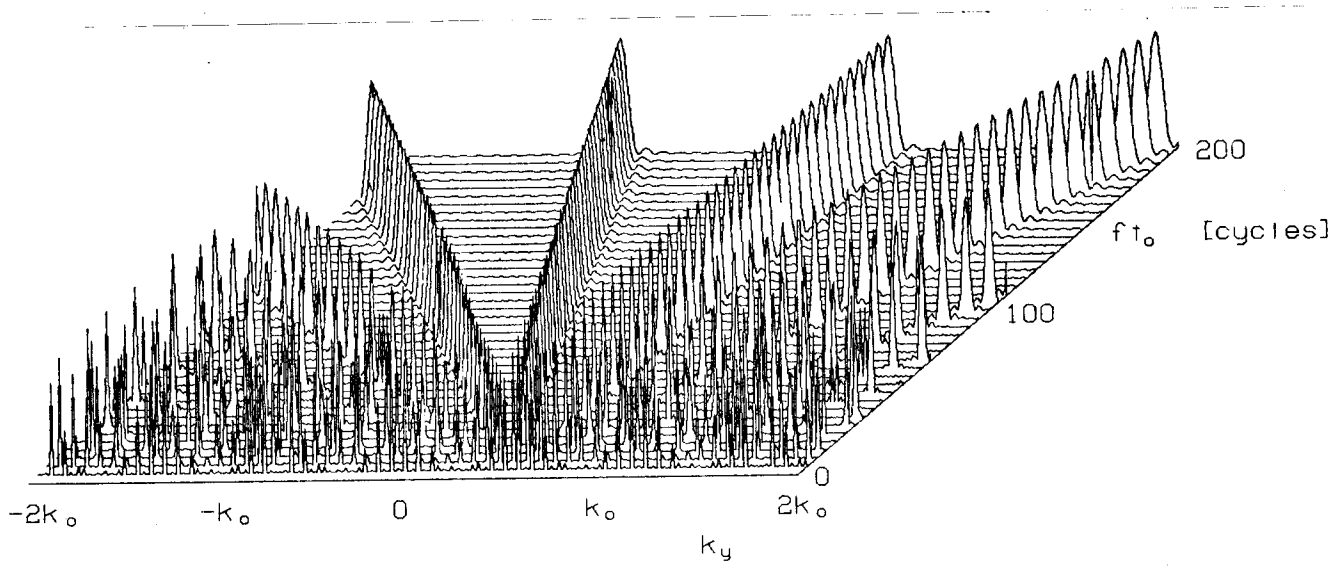

FIG. 8. $F_n(k)$, $(n = 1)$, UOS spacing, $N = 16$.

Referring to equations (12) and (13), F peaks whenever Φ is an integer multiple of 2π. The case $\Phi = 0$, i.e $k = nk_0/2$, cannot be avoided, as observed before. The "$\Phi \neq 0$" cases can be avoided in two ways. The expensive one is to make N big, the other way is to perturb the exact UOS spacing, i.e., to take j not evenly spaced in the summation (12).

Choosing offsets with slightly perturbed UOS so that there are no overlaps in the j's of equation (12), we get Figure 9.

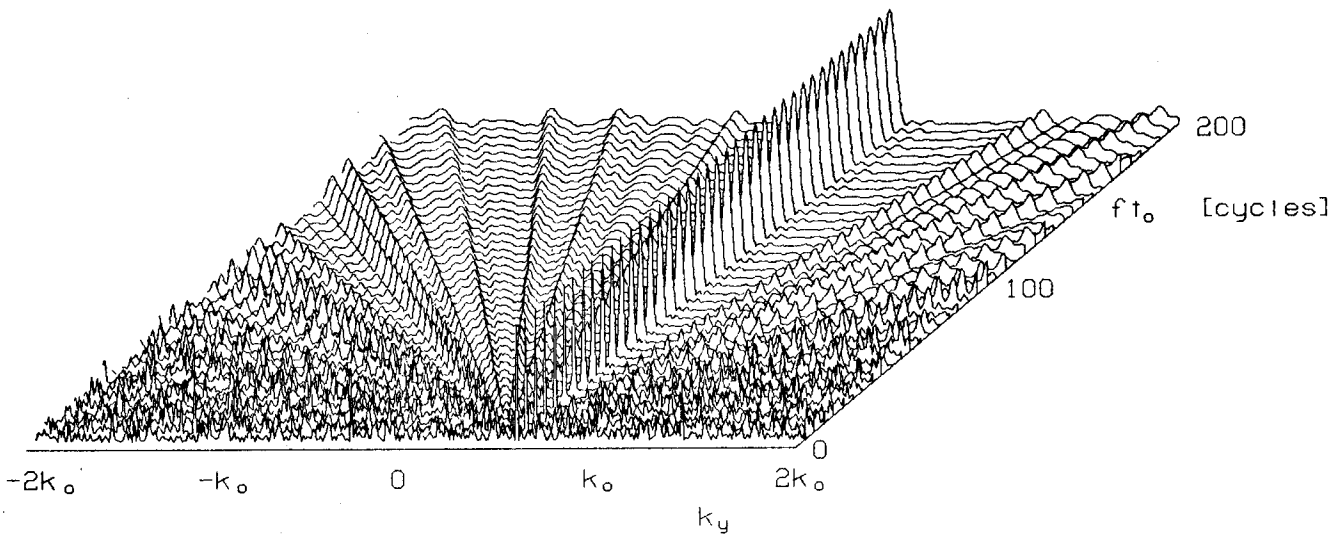

FIG. 9. $f_1(k,\omega t_0)$, $(n = 1)$, $N = 16$. Perturbed UOS stacking.

As we saw in equation (9) the amount of aliasing of the data determines the quality of the stack; if the data are not aliased at all, the shape of $F_n(k)$ for $n \neq 0$ is irrelevant. Suppose, however, that the midpoint sampling is 25 m and the spectrum of the data is given by Figure 10. The Nyquist is 0.02 m^{-1} therefore the data are aliased.

Assuming normalized summation over offset, the stack is given by:

$$Stack(k) \;=\; P_0(k) \;+\; \sum_{n=1}^{\infty} \Big[P_0(k-nk_0)F(k) + P_0(k+nk_0)F(k)_{-n} \Big]$$

From Figure 10 it is seen that the summation can be truncated at $n = 2$ and that most of the noise comes from $|n| = 1$. The spectrum of the $|n| = 1$ noise is given by:

$$\Big|P_0(k-nk_0)\Big|^2 \Big|F_n(k)\Big|^2 + \Big|P_0(k+nk_0)\Big|^2 \Big|F_{-n}(k)\Big|^2$$

The expected spectra of the noise, within the aliasing model of Figure 10, obtained with different processing are shown in Figures 11 through 14.

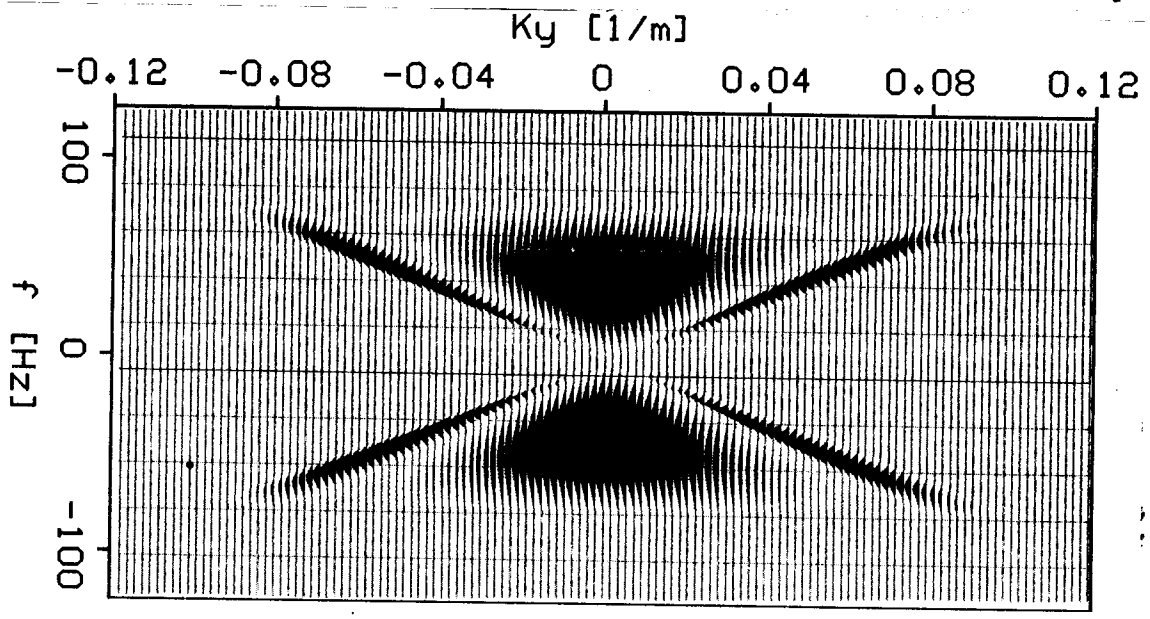

FIG. 10. Typical spectrum.

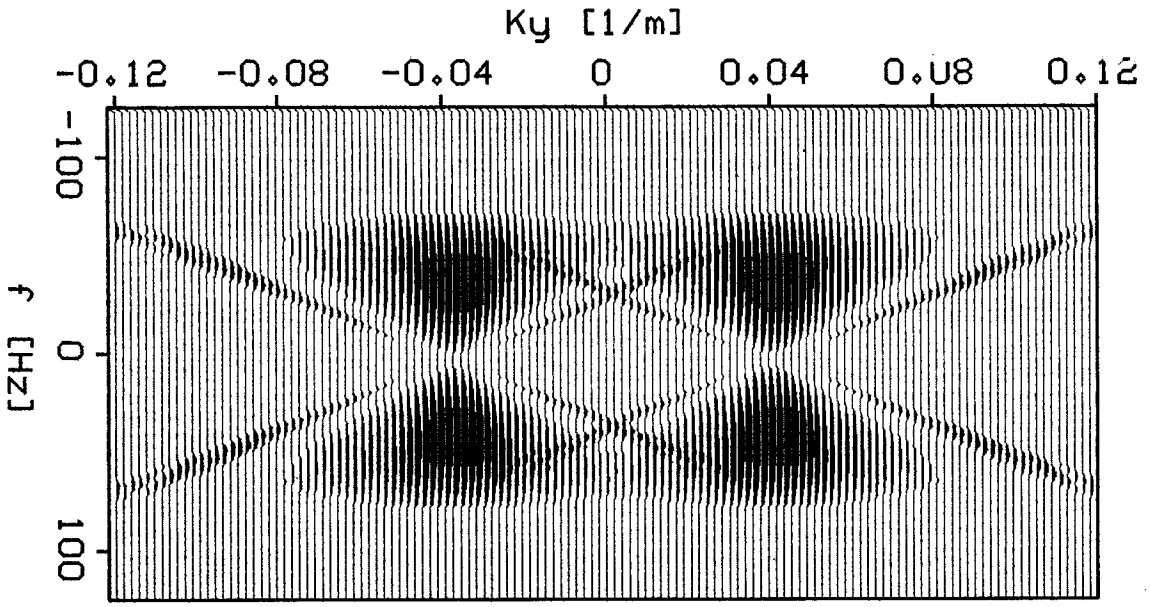

FIG. 11. Aliasing noise for $n = \pm 1$. No DMO, uniform offset spacing (conventional). Noise energy = 155 (in relative units).

Why UOS is a good spacing

Using Figures 6 ,8 and 9, we have shown that UOS spacing is better than uniform offset spacing; in this section we shall see why. Define $y_h = nk_0/\omega t_0 h^2$, then equation (10) will read:

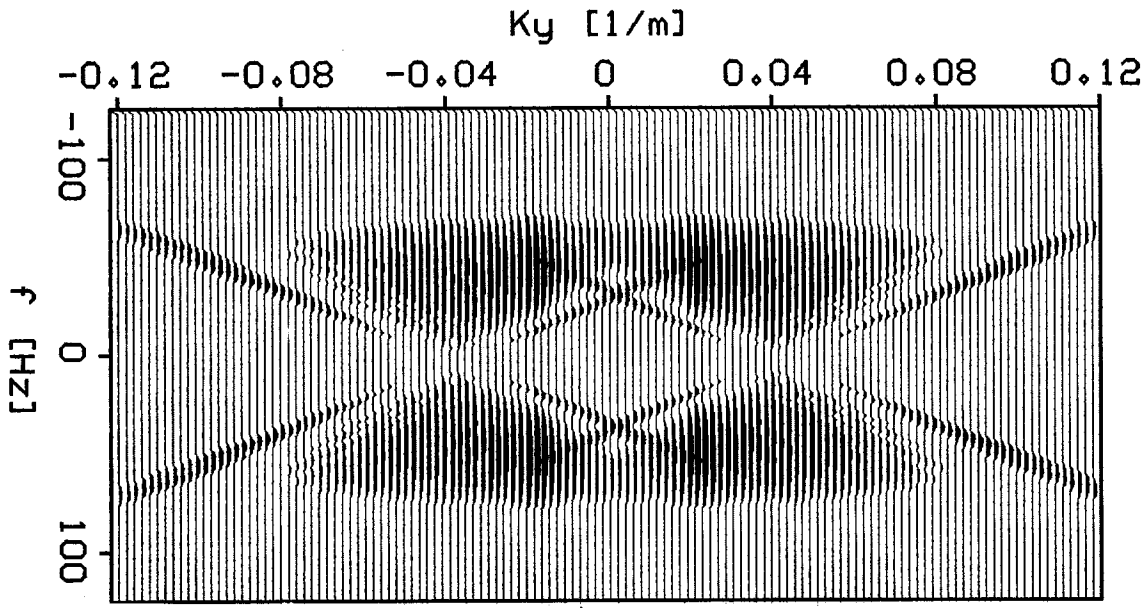

FIG. 12. Noise for $n = \pm 1$. DMO, uniform offset spacing. Noise energy = 31.

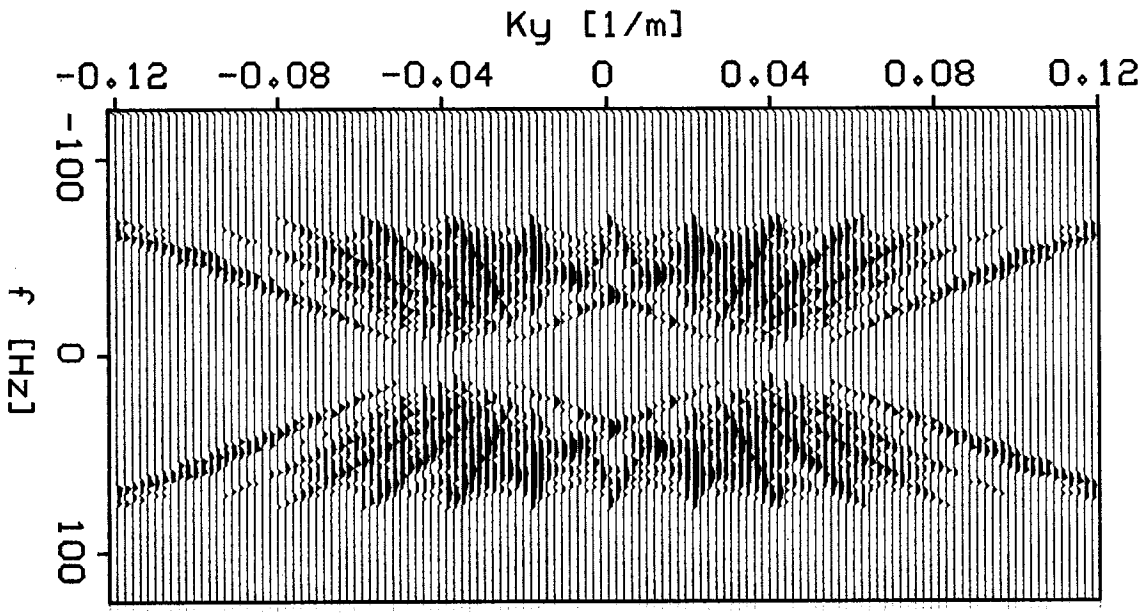

FIG. 13. Noise for $n = \pm 1$. DMO, UOS stack. Noise energy = 22.

$$F_n(k) = \sum_h \exp\left[-i\, y_h n \frac{k_0}{2}\right] \exp\left[i\, y_h k\right]$$

Transforming back to the y domain:

$$f_n(y) = \sum_h \exp\left[-i\, y \frac{n k_0}{2}\right] \cdot \delta(y - y_h)$$

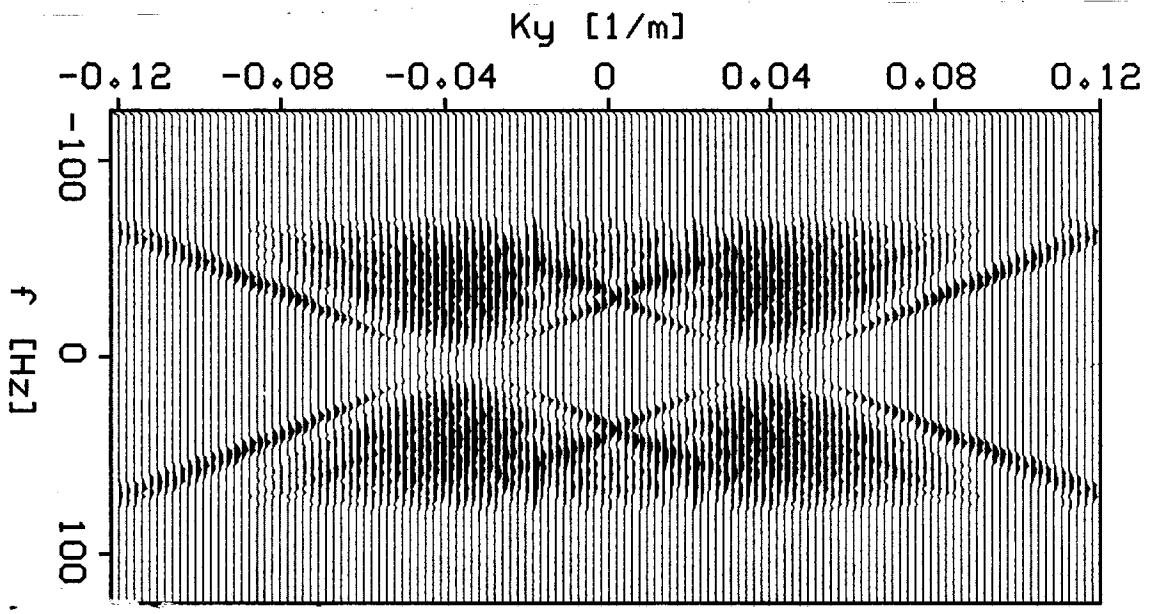

FIG. 14. Noise for $n = \pm 1$. DMO, perturbed UOS stack. Noise energy = 18.

We see that $f_n(y)$ is a train of spikes with unit amplitudes and linear phase shifts. This phase term shifts the spectrum so that it peaks around $k = nk_0/2$, as we know. To make the peak as narrow as possible, the spikes of $f_n(y)$ should, according to the uncertainty relation, be as dispersed as possible. Since y_h is proportional to h^2, this implies optimality of UOS. If the number N of offsets is high enough, the additional peaks due to aliasing in offset space (i.e. $\Phi = 2\pi$ or multiple) can be pushed further away along the wavenumber axis, generating Figure 5. If, on the other hand, we wish to keep N small, so that we carry out DMO on a limited set of offsets only, then an easy way to limit offset aliasing is to slightly perturb the UOS order. This explains why Figure 9 gives the best results for $N = 16$, up to now.

Conclusions

We have seen that the main advantage in carrying out DMO lies in the reduction of coherent noise like cable noise and aliasing. The signal distortion is also reduced, but this effect is slight and could also be carried out after stack. On the other hand, noise reduction needs only approximate DMO. The suggested process is therefore:

1) Carry out a cheap dip moveout, considering the quality of the data.
2) Velocity analysis, NMO and optimal stack.
3) Post stack residual dip moveout.
4) Migration.

If an accurate velocity analysis is desired the DMO correction should be carried out more carefully.

REFERENCES

Bolondi, G., Loinger, E. and Rocca, F., 1982, Offset continuation of seismic sections, To appear in Geophysical Prospecting, Presented at the EAEG 43rd Meeting, Venice, 1981.

Deregowski, S.M. and Rocca, F., 1981, Geometrical optics and wave theory of constant offset sections in layered media, Geophysical Prospecting, v. 29, p. 374 - 406. (Also SEP 16, p. 25 - 53.)

Hale, D., 1982, Migration of non-zero-offset sections, SEP 30, p. 29-41.

Larner, K., Chamber, R. and Yang, M., 1981, Towards an understanding and suppression of coherent noise in marine data, presented at the 51st SEG Meeting, Los Angeles, 1981.

Levin, F.K., 1971, Apparent velocity from dipping interface reflections, GEOPHYSICS v. 36, p. 510 - 516.

Ottolini, R., 1981, Migration before stack by transforming into snell trace coordinates, SEP 28, p. 121-138.

Sherwood, J.W.C., Schultz, P.S. and Judson, J.R., 1976, Some recent developments in migration before stack. Released by Digicon, Inc.

Yilmaz, O. and Claerbout, J.F., 1980, Prestack partial migration, GEOPHYSICS v. 45, p. 1753-1779.